Published in IET Image Processing
Received on 28th August 2009
Revised on 19th February 2010
doi: 10.1049/iet-ipr.2009.0239

Special Issue on Computer Graphics And Multimedia Security

ISSN 1751-9659

Robust discrete wavelet–fan beam transforms-based colour image watermarking

D. Dejey R.S. Rajesh

Department of Computer Science and Engineering, Manonmaniam Sundaranar University, Tirunelveli, Tamil Nadu, India
E-mail: dejeytilak@gmail.com

Abstract: Combined discrete wavelet transform–fan beam transform (DWT–FBT) has been explored as a new possible domain for colour image watermarking. The two schemes proposed in the combined domain are (i) wavelet fan beam watermarking on luminance and chrominance and (ii) wavelet fan beam watermarking on chrominance alone. After the application of DWT on the host image and after careful selection of the suitable band of wavelet coefficients for applying FBT, watermarking is done by altering the fan beam transformed coefficients. The schemes proposed achieve a high data embedding capacity in addition to robustness to attacks and produce watermarked images of high quality. Results of the proposed schemes are compared with the two existing DWT–discrete cosine transform watermarking schemes to show its effectiveness.

1 Introduction

With the recent proliferation of the Internet, the issue of protecting the copyrights of digital content has become more and more important. The new technology of digital watermarking has been advocated by researchers as the best solution to the multimedia copyright protection problem. Digital watermarking is a technique to embed generally invisible data within the multimedia content. Digital image watermarking is implemented in two ways, namely in spatial domain and in frequency domain. When compared to spatial-domain techniques, frequency-domain watermarking techniques proved to be more effective in achieving the imperceptibility and robustness requirements of digital watermarking algorithms [1]. The commonly used frequency-domain transforms are the discrete cosine transform (DCT), discrete Fourier transform (DFT), discrete wavelet transform (DWT) and so on. However, DWT has been used in digital image watermarking more frequently than other transforms because of its excellent spatial localisation and multi-resolution characteristics, which are similar to the theoretical models of the human visual system (HVS) [2]. In this paper, it is shown that the combined discrete wavelet transform–fan beam transform (DWT–FBT) domain can have further improvement in robustness than traditional DWT-based digital image watermarking algorithms.

Several digital image watermarking algorithms based on combining the two transforms have been proposed in the literature and some are as follows: Al-Haj [1] has proposed a watermarking scheme, wherein DWT and DCT are combined and watermarking is done by altering the wavelet coefficients of carefully selected DWT sub-bands, followed by the application of the DCT on the selected sub-bands. This combined DWT–DCT watermarking algorithm's imperceptibility performance and robustness are better than the performance of the DWT only approach. The digital watermarking scheme proposed by Tripathi *et al.* [3] uses the properties of DCT and DWT to achieve almost zero visible distortion in the watermarked images. Also, this technique uses a linear relation between the transform coefficients of the watermark and a security matrix for spreading, embedding and extracting the multiplicative watermark and is shown to be robust to some attacks. The DWT–DCT-based digital watermarking technique developed by Emek and Pazarci [4] uses a DWT beforehand to provide higher robustness and imperceptibility rather than inserting the watermark to the DCT mid-frequency coefficients. The robustness of this approach is achieved by the ability to increase the energy of the watermark, which is done by locally exploiting the properties of the HVS such that the human eye will not notice it. Furthermore, imperceptibility is also improved due to the DWT. Jiansheng *et al.* [2] have proposed a watermarking scheme using the block technology and watermarking signal is embedded into the high-frequency band of wavelet transformation domain. Before embedding, this watermark image has been discrete cosine transformed in order to improve robustness and has proven to keep the image quality well and robust to many common image processing operations. A blind DWT–DFT composite image watermarking algorithm that is robust against both affine transformation and JPEG compression has been proposed by Kang *et al.* [5]. A spread spectrum-based informative watermark with a training sequence is embedded on the coefficients of the LL sub-band in the DWT domain, whereas a template is embedded on the middle frequency components in the DFT domain to obtain the parameters of an affine transform and to convert the image back to its original shape during watermark

extraction. A translation registration using the training sequence embedded in the DWT domain is performed to extract the informative watermark. The watermarking algorithm based on joint DWT–DCT transformation proposed by Kasmani and Nilchi [6] provides imperceptibility as well as higher robustness against common signal processing attacks. Here, a binary watermarked image is embedded in certain sub-bands of a three-level DWT transformed host image. Then, DCT transform of each selected DWT sub-band is computed and the PN-sequences of the watermark bits are embedded on the coefficients of the corresponding DCT middle frequencies and the correlation between mid-band coefficients and PN-sequences is calculated to determine the watermarked bits.

In the field of watermarking, since the current trend is to consider both the luminance and chrominance content for watermarking [7], an attempt is made in this paper to include the luminance content along with the chrominance content for watermark embedding. The spin current DFT-based approach proposed by Tsui *et al.* [7] uses only the chrominance content for watermarking. Although the quaternion Fourier transform-based watermarking [7] proposed by them uses both the luminance and chrominance, it is highly computationally inefficient. In this paper, the combined DWT–FBT domain has been investigated as a new possible domain for watermarking. After the application of DWT on the host image and after careful selection of the suitable band of wavelet coefficients for applying FBT, watermarking is done by altering the fan beam transformed coefficients. Normally projection data of single and multiple sources are used for reconstructing distorted images. But in this paper, we utilise the fan beam projection data for embedding the watermark. It is because the voluminous projection data maximises the area for embedding the watermark and a large amount of information can be embedded. Also, this does not affect the perceptivity and the watermark embedded is robust to large classes of attacks.

A related work is done by Cai and Du [8], wherein fusion of radon transform and Fourier transform has been performed for watermarking which is invariant to rotation, scale and translation. To represent an image, the radon transform takes multiple, parallel beam projections of the image from different angles by rotating the source around the centre of the image. Previous researches have faced the problem of obtaining a high resolution because of using parallel projection. This is due to the fact that the parallel projection method limits the number of measurements to the number of sensors being used [9]. Hence, in our proposed schemes fan beam projection is used rather than parallel projection. Fan beam projection is advantageous because it completely covers the object to be imaged. Also, it is noted for its speed as obviously, multiple detectors of the fan beam can gather data faster than a single detector [10]. Our earlier work on colour image watermarking based on the fan beam projection showed the best robustness against attacks [11] and other works on watermarking colour images in the wavelet domain resulted in watermarked images with very good quality. This led to the idea of combining wavelet with FBT so that they would compensate the drawbacks of each other, resulting in an effective watermarking scheme. Thus, the proposed techniques in the combined DWT–FBT domain attempt to find a tradeoff between the three conflicting requirements of any watermarking scheme, namely capacity, robustness and imperceptibility. With the available literature, it is found that this combined domain has not been attempted so far in the field of watermarking.

Section 2 describes the background of DWT and FBT. The proposed technique is presented in Section 3 and experimental results are discussed in Section 4. Section 5 concludes the paper with future scope.

2 Background

2.1 Discrete wavelet transform

With DWT, a time-scale representation of the digital signal is obtained using digital filtering techniques and is computed by successive low-pass and high-pass filtering of the discrete time-domain signal, as shown in Fig. 1. In the figure, the signal is denoted by the sequence $x(n)$, where n is an integer. The low-pass filter is denoted by $g(n)$, whereas the high-pass filter is denoted by $h(n)$.

At each decomposition level, the half-band filters produce signals spanning only half the frequency band. This doubles the frequency resolution, as the uncertainty in frequency is reduced by half. In accordance with Nyquist's rule, if the original signal has a highest frequency of π, which requires a sampling frequency of 2π radians, then it now has a highest frequency of $\pi/2$ radians. It can now be sampled at a frequency of π radians, thus discarding half the samples with no loss of information. This decimation by two halves the time resolution, as the entire signal is now represented by only half the number of samples. Thus, while the half-band low-pass filtering removes half of the frequencies and thus halves the resolution, the decimation by two doubles the scale. A single-level decomposition can mathematically be expressed as in (1)

$$y_{\text{high}}[k] = \sum_n x(n) \times g(2k - n)$$
$$y_{\text{low}}[k] = \sum_n x(n) \times h(2k - n) \tag{1}$$

With this approach, the time resolution becomes arbitrarily good at high frequencies, whereas the frequency resolution becomes arbitrarily good at low frequencies. The filtering and decimation process is continued until the desired level is reached. The maximum numbers of levels depend on the

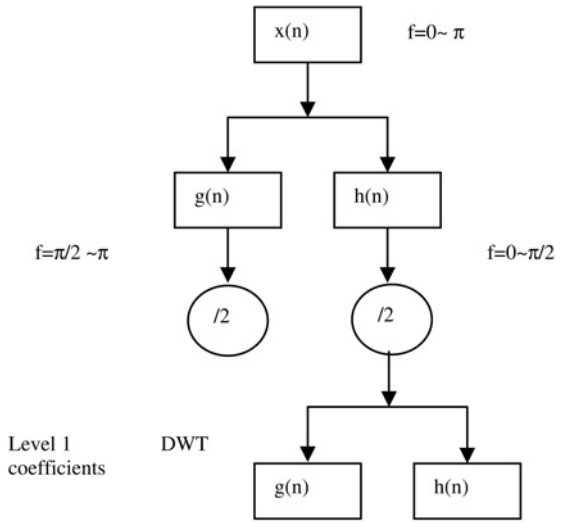

Fig. 1 *Single-level DWT decomposition*

doi: 10.1049/iet-ipr.2009.0239

length of the signal. The DWT of the original signal is then obtained by concatenating all the coefficients, $y_{high}[k]$ and $y_{low}[k]$, starting from the last level of decomposition.

In a two-dimensional DWT, a single-level decomposition on an image produces four bands of data, one corresponding to the low-pass band (LL) and two others corresponding to mid-frequency bands namely horizontal (HL), vertical (LH) and one high-pass band namely diagonal (HH). The reason for single-level wavelet decomposition is that the area for embedding the watermark is maximised [12]. The hierarchical image representation due to the multi-resolution characteristics of the DWT domain allows the insertion of the watermark in any band. Generally, if the watermark is embedded in the low-resolution sub-band LL, it is robust to attacks but causes degradation in the quality of the image. On the other hand, a small modification in the HH sub-band is not perceived by human eyes but the robustness is compromised. Based on these considerations, usually embedding is performed in the LH and HL sub-bands [13]. The algorithm proposed by Shieh *et al.* [14] applies the genetic algorithm for choosing the appropriate DCT frequency bands for embedding the watermark that can watch both the watermarked image quality and the robustness under certain attacks in every training iteration. Since in our earlier work [15], among the mid-frequency bands, HL band provided better results than the LH band, it is chosen for watermark embedding in the proposed schemes.

2.2 Imaging geometry and the FBT

A projection of a two-dimensional function $f(x, y)$ is a set of line integrals from which data can be produced by radiating from single and multiple sources. Projection of an image can be computed along any angle θ. In parallel beam geometry, each projection is formed by combining a set of line integrals through an image at a specific angle and there are equal number of n emitters and n sensors. Another geometry that is commonly used is the *fan beam* geometry, in which there is one emitter and n sensors.

Let f be an integral real function on the R^2 plane. Let S be a point called source point and $\boldsymbol{v}_\theta$ be a unit vector in the direction $\theta \in [0, 2\pi]$ on the plane. Consider the integrals of f along half lines starting from S in direction $\boldsymbol{v}_\theta$, then

$$[Rf](S, \theta) = \int_0^\infty f(S + u \cdot \boldsymbol{v}_\theta)\, du \tag{2}$$

The transformation defined by (2) is called the fan beam projection of f taken from the point S in the direction θ [16]. FBT computes the line integrals along paths that radiate from a single source. To represent an image, it performs multiple projections of the image from different angles by rotating the source around the centre of the image. The fan beam projection computes the projection data as sinogram. In fan beam geometry, the detectors are arranged on a circular arc and the angular increments of the source are assumed to be equal.

Let $\rho(\alpha, \beta)$ denotes a fan beam projection, where α is the angular position of a particular detector measured with respect to the centre ray and β is the angular displacement of the source measured with respect to y-axis. A ray in the fan beam can be represented as a line $L(\rho, \theta)$ in the normal form. The parameters of the line $L(\rho, \theta)$ are related to the parameters of the fan beam ray by (3) and (4)

$$\theta = \beta + \alpha \tag{3}$$

and

$$\rho = D \sin \alpha \tag{4}$$

where D is the distance from the centre of the source to the origin of the xy plane [17]. This is shown in Fig. 2.

In the fan beam calculation, the centre of rotation is the centre of the image and is defined in (5) as

$$\text{Center} = \text{size}(f(x, y) + 1)/2 \tag{5}$$

where size $(\cdot)$ returns the size of the image $f(x, y)$ and its lower precision value is taken for the centre of rotation calculation. D is the distance in pixels from the single source point to the centre of rotation. It must be large enough to ensure that the single source point is outside the image at entire rotation angles, which is ranged from 0 to 359°. The distance D should be larger than half the image diagonal dimension. This is described in (6) as

$$D = \sqrt{\text{width}(f(x, y))^2 + \text{height}(f(x, y))^2} \tag{6}$$

After applying the fan beam projection, the resultant data contain row and column of sinogram from the image $f(x, y)$. The row data contain the number of sensor points by calculating how many beams are needed to wrap the entire image for any rotation angle. The number of column of fan data is determined by incrementing the fan rotation. It may be one degree and fan beam data can have 360 columns.

Fan beam can be controlled by various parameters such as rotation increment, sensor geometry and sensor spacing. The rotation increment has a positive real scalar, measured in degrees, sensor geometry defines either line sensors or arc sensors and sensor spacing is used to define the spacing of the fan beam projections. If sensor geometry is 'arc' then sensor spacing has the angular spacing in degrees, else linear spacing in pixels [18].

However, with the proposed watermarking scheme, to the selected mid-frequency band after wavelet decomposition,

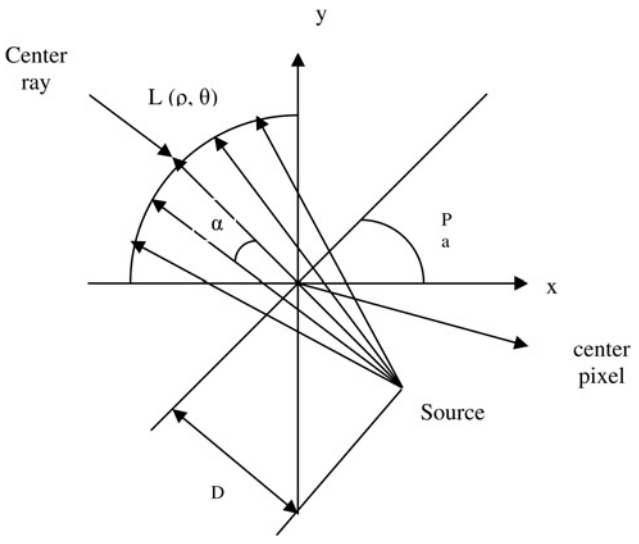

Fig. 2 *Basic fan beam geometry*

FBT is applied. Then, the fan beam projection data are extracted from the image and the watermark is embedded in it. Since the detectors are arranged in a circular arc and at angular increments, it yield multiple projections, which pave the way to maximise the capacity of the watermark.

2.3 Colour space

Colour transformation deals with processing the components of a colour image within the context of a single colour model as composed conversion of those components between models. In order to maintain a high degree of colour consistency, the model of choice for many colour management systems is the CIE $L^*a^*b^*$ model, also called as CIELAB. The advantage of $L^*a^*b^*$ colour space is its colorimetric, perceptually uniform and device independent nature. Also, its gamut encompasses the entire visible spectrum and can represent accurately all the colours. $L^*a^*b^*$ colour space decouples intensity and colour, making it useful in image manipulation applications [19]. Hence, in the proposed work, $L^*a^*b^*$ space is used for watermarking since it models human perception of colours. As it is not a directly displayable format, the watermarked image is converted back to red–green–blue (RGB) colour space.

3 Proposed DWT–FBT-based colour image watermarking algorithms

Initially, the original image I of size $N \times N$ is converted to $L^*a^*b^*$ colour space. For the wavelet fan beam watermarking on chrominance (WFWC) scheme, the colour information in $L^*a^*b^*$ space is then coded as complex number Z of the form as proposed by Tsui *et al.* [7]. This is shown in (7) as

$$Z = a + \mathrm{j}b \tag{7}$$

For the wavelet fan beam watermarking on luminance and chrominance (WFWLC) scheme, the luminance and the colour information are coded as complex number Z of the form given by (8)

$$Z = (L + a) + \mathrm{j}b \tag{8}$$

where L corresponds to the luminance; a and b correspond to the chrominance content of the image in $L^*a^*b^*$ space. The watermark (W_E) to be embedded is a binary pattern. Any video, audio or image can be used as the watermark and it has to be converted to binary bit stream. The embedding and the extraction mechanisms for both WFWC and WFWLC schemes are one and the same and are discussed in the following section.

3.1 Watermark embedding

The DWT is applied to the magnitude of the chrominance content of the original colour image for WFWC as shown in (7) and to the magnitude of both the luminance and chrominance content of the colour image as shown in (8) for WFWLC. A single-level DWT decomposition produces four bands of data, and to the wavelet transformed coefficients in the HL band, FBT is applied. After applying the FBT, the resultant data contain row and column of sinogram of the image. This is divided into blocks of size 8×8. Only those 8×8 blocks which have non-zero values are chosen for embedding the watermark. The watermark bit is embedded into the transformed coefficient in each 8×8 non-zero block as shown in (9)

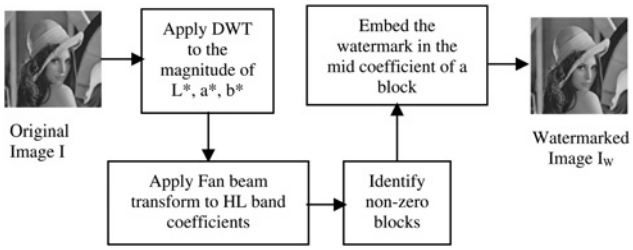

Fig. 3 *Watermark embedding using the proposed DWT–FBT watermarking*

$$F(f_1, f_2) = \begin{cases} F(f_1, f_2) \pm \beta m(k) & \text{if } W(k) = 1 \\ F(f_1, f_2) & \text{if } W(k) = 0 \end{cases} \tag{9}$$

where $F(f_1, f_2)$ is the fan beam transformed coefficient in any 8×8 non-zero block, β is the watermark strength, $m(k)$ is the mid-coefficient in any kth 8×8 block and $W(k)$ is the watermark bit and k is the index of the watermark to be embedded. Depending on the perceptual requirement, the value of β is varied. Then, an inverse FBT is applied. The original DWT coefficients in the HL band are replaced by the watermarked coefficients and inverse DWT is applied. Watermarked image I_W is obtained by converting the resultant $L^*a^*b^*$ into RGB space. The watermark embedding framework is shown in Fig. 3.

3.2 Watermark extraction

To extract the embedded watermark, the original image I and the watermarked image I_W or probably the attacked image are needed. The values of $F(f_1, f_2) \pm \beta m(k)$ are calculated from the original image. Then, a distance comparison is made to the coefficients extracted from the watermarked image/attacked image. If the coefficients extracted from the watermarked image are closer to those values computed from the original image, then the bit in the extracted watermark W_X is '1'. Otherwise, the bit extracted is assumed to be '0'. The watermark extraction framework is shown in Fig. 4.

4 Experimental results

In this section, the effect of the proposed DWT–FBT image watermarking schemes, WFWC and WFWLC implemented using MATLAB 7.2, is presented. The fidelity criteria and robustness of the proposed watermarking schemes are evaluated with standard test images available in the USC-SIPI image database [20] and those discussed in tables are shown in Fig. 5. The proposed methods are compared with a combined DWT–DCT approach proposed by Al-Haj [1] and a joint DWT–DCT-based approach proposed by Kasmani and Nilchi [6]. Since our work is for colour images, for uniformity sake, both DWT–DCT approaches are applied to colour images by considering the blue channel alone for watermarking as it is learnt from the literature that the HVS is less sensitive to blue [21]. In Al-Haj's method, after two levels of wavelet decomposition, the HL band is divided into 4×4 blocks wherein DCT is applied. Watermarking is done with a watermarking strength $\alpha = 25$ on the mid-band coefficients. Using this approach, on an image with dimensions 256×256, only 256 bits of

doi: 10.1049/iet-ipr.2009.0239

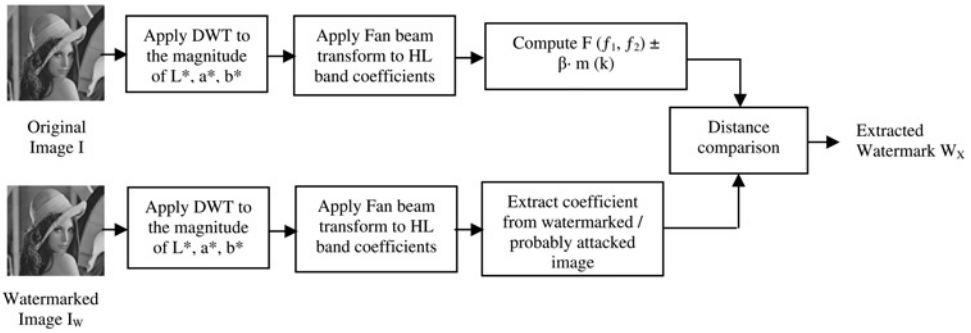

Fig. 4 *Watermark extraction using the proposed DWT–FBT watermarking*

information can be embedded with one bit per 4 × 4 block. In the other method proposed by Kasmani and Nilchi [6] taken for our comparison, the bands chosen for watermarking are HL_{13}, LH_{13}, HL_{23} and LH_{23}, which are obtained after three levels of wavelet decomposition. To these bands, DCT is applied on 4 × 4 blocks and watermarking is done on mid-band coefficients. Watermarking is done with a watermarking strength $\alpha = 25$. In this approach also, only 256 bits can be embedded on an image of size 256 × 256 with one bit per 4 × 4 block. Comparison results of the existing schemes and the proposed schemes are discussed in the following sections.

In the experiments, with the proposed schemes, any image of size $N \times N$ is first subjected to a single-level DWT decomposition using Haar filter. This results in four bands of data with $N/2 \times N/2$ samples. Among the four bands of data, the HL band is chosen for further processing. Now, to the $N/2 \times N/2$ samples of HL band, the FBT is applied to obtain row and column of sinogram in which the watermark is embedded. The important parameters to be specified for the FBT are the distance parameter D, the rotation increment, the sensor geometry and the sensor spacing (d). In the experiments, the rotation angles equally change from 0 to 359°; D is computed using (6); rotation increment which is measured in degrees is a positive real scalar specifying the increment of the rotation angle of the fan beam projections and is set to the default value = 1; the sensor spacing is a positive real scalar specifying the spacing of the fan beam sensors. Interpretation of its value depends on the setting of sensor geometry which defines the angular spacing in degrees and is set to 'arc' by default.

For instance, a single-level DWT decomposition using Haar filter on an image of size 256 × 256 results in a HL band of size 128 × 128 which is fan beam transformed. After performing FBT, the resultant fan beam projection data of size 544 × 360 is extracted from the image, where the sensor spacing is set as 0.05. It means that the fan beam projection provides 544 sensors and 360° rotation angles. The number of sensors is determined by the fan beam sensor spacing. In the resultant fan beam projection data, s non-zero blocks of size 8 × 8 are identified for embedding the watermark and in this case where sensor spacing = 0.05, 2650 non-zero blocks are identified for Lena image and a watermark of such a length is embedded in those blocks. Watermarking is done as in (9) and that to in location (5, 5) which is assumed to the mid-coefficient in a block and is chosen after conducting many experiments. The other important parameter used in the embedding procedure is the value of β, which is the embedding strength that is fixed depending on the level of imperceptibility needed. In the experiments, $\beta = 0.001$ is used. This value of β is also used as the threshold for recovering the embedded watermark by comparing the watermarked image with the original during the watermark extraction phase. The original and the watermarked images using WFWC and WFWLC watermarking schemes are shown along with the amount of information embedded and the associated peak signal-to-noise ratio (PSNR) in Fig. 6.

The sensor spacing (d) plays an important role in our embedding phase as it decides the amount of information to be embedded in the image. Its value is chosen after an analysis is made on varying the values of sensor spacing on Lena image for various image dimensions. This is shown in Table 1.

From Table 1, it is learnt that (i) PSNR of the watermarked image is not affected by increasing or decreasing the value of sensor spacing, d; (ii) While d value is reduced, the processing time for watermarking increases for images irrespective of dimensions; (iii) d has an impact on the amount of information embedded, that is, the watermarking

Fig. 5 *Test images*

a Dish
b Goldhill
c House
d Lena

Fig. 6 *Original and the watermarked images using WFWC and WFWLC watermarking schemes*

a Original image
b Watermarked image using WFWC
c Watermarked image using WFWLC (Image size: 256 × 256; bits embedded: 2650 bits; PSNR: 54.16 and 50.45 dB, respectively)

capacity and in fact, the huge watermarking capacity of the proposed watermarking schemes are due to the sensor spacing of the FBT which provides samples for each rotation angle, thus maximising the area for embedding the watermark; (iv) $d = 0.05$ is optimal for all image sizes and (v) $d < 0.05$ will always make watermarking imperceptible irrespective of the image size.

Hence, for further analysis and robustness tests, the image dimension chosen for consideration is 256 × 256 and the sensor spacing is taken to be 0.05, as it is optimal in terms of watermarking capacity and processing time.

4.1 Fidelity criteria

When the level of information loss is expressed as a function of original image and watermarked image, it is said to be based on objective fidelity criterion [19]. The root mean square error is one such best criteria and is given in (10)

$$\text{RMSE} = \sqrt{\frac{1}{w \times h}\sum_{j=0}^{h-1}\sum_{i=0}^{w-1}((\Delta R_{ij})^2 + (\Delta G_{ij})^2 + (\Delta B_{ij})^2)} \tag{10}$$

where R_{ij}, G_{ij} and B_{ij} are the red, green and blue values of the pixel and w and h are the width and height of the image.

To evaluate the fidelity of the watermark, the PSNR is used and it is measured in (11) as

$$\text{PSNR} = 10 \log_{10}\left(\frac{3 \times 255^2}{\text{RMSE}}\right) \tag{11}$$

Table 1 Analysis made on fan beam sensor spacing d on Lena image of various sizes

Image size	Fan beam sensor spacing *d*	Bits embedded	PSNR (in dB)	Processing time (in seconds)
128 × 128	0.10	1433	43.64	2.94
	0.05	2904	43.66	4.32
	0.01	14 694	42.5	33.8
256 × 256	0.10	1410	50.29	3.89
	0.05	2857	50.45	5.11
	0.01	14 413	38.61	32.74
512 × 512	0.10	1396	55.21	6.57
	0.05	2831	55.42	7.68
	0.01	14 300	38.25	35.25

The typical value for PSNR is between 30 and 50 dB and the higher, the better.

A huge amount of information can be embedded with the proposed schemes depending on the fan beam sensor spacing and the distance of the vertex from the centre of the image. The PSNR and number of bits embedded are tabulated for the proposed schemes in Table 2 for images of size 256 × 256 along with that for existing Al-Haj's DWT–DCT scheme (2007) [1] and Kasmani and Nilchi DWT–DCT scheme (2009) [6] with the condition that the bit error rate (BER) is zero under no attack. BER is defined as the ratio between the number of incorrectly extracted bits and the length of the watermark.

From Table 2, it can be noticed that for the proposed schemes, more than 2600 bits of information can be embedded which is ten times more than that of the existing DWT–DCT schemes where only 256 bits can be embedded. The PSNR for the proposed schemes is more than 50 dB for images of size 256 × 256, whereas for both the existing DWT–DCT, it is comparatively low. To have a uniform benchmark, attempt is made to embed more information with both the DWT–DCT schemes. In the experiments, 1024 bits (4 bits per 4 × 4 block) are embedded with both the schemes on an image with dimensions 256 × 256. It can be seen that for Lena image that the PSNR drops down to 36.30 from 42.32 for Al-Haj's DWT–DCT scheme [1] with visible distortion as shown in Fig. 7*a* by circled area and also drops down to 27.12 from 40.95 for Kasmani and Nilchi [6] DWT–DCT scheme with visible distortions as shown in Fig. 7*b*. On embedding even more number of bits, the PSNR is even poorer with more visual degradation in the watermarked image. Also, it does not guarantee zero BER under no attack. This means that both the existing DWT–DCT

Table 2 Bits embedded and PSNR obtained when BER is zero under no attack for WFWC, WFWLC and existing DWT–DCT schemes

Image	Approach	Bits embedded	PSNR (in dB)
Dish	WFWC	2791	49.57
	WFWLC	2791	48.01
	Al-Haj's DWT–DCT	256	35.28
		1024	29.26
	Kasmani *et al.* DWT–DCT	256	36.31
		1024	22.14
Goldhill	WFWC	2650	54.77
	WFWLC	2650	48.46
	Al-Haj's DWT–DCT	256	33.80
		1024	27.78
	Kasmani *et al.* DWT–DCT	256	34.15
		1024	21.39
House	WFWC	2650	53.87
	WFWLC	2650	52.08
	Al-Haj's DWT–DCT	256	32.23
		1024	27.21
	Kasmani *et al.* DWT–DCT	256	37.20
		1024	30.39
Lena	WFWC	2650	54.16
	WFWLC	2650	50.45
	Al-Haj's DWT–DCT	256	42.32
		1024	36.30
	Kasmani *et al.* DWT–DCT	256	40.95
		1024	27.12

doi: 10.1049/iet-ipr.2009.0239

Fig. 7 *Lena images watermarked with 1024 bits*
a Using Al-Haj's scheme
b Using Kasmani *et al.* scheme showing visible distortion

approaches fail to meet the minimum requirement of any watermarking scheme to have zero BER under no attack when embedding more number of bits. Hence, it is clear that the proposed DWT–FBT watermarking domain maximises the watermarking capacity, perhaps the watermark embedded being imperceptible resulting in watermarked images of very good quality.

Also, from Table 2 it is observed that there is significant increase in image quality while considering the chrominance alone for watermarking than both luminance and chrominance in the proposed DWT–FBT domain. The experiment is also conducted for images of sizes 64 × 64, 128 × 128, 256 × 256, 512 × 512 and the PSNR is always the best irrespective of the image size as observed from Table 1. It can also be seen that the imperceptibility criterion of the proposed watermarking schemes is the highest when compared to [1, 6]. It is partly because of DWT with which both coarse and fine resolution approximations of the original image can be extracted even after embedding the watermark [19] and partly due to the FBT, which spreads the watermark covering the entire image.

4.2 Robustness of the watermark

In order to prove the robustness of the proposed DWT–FBT watermarking scheme against attacks, a series of experiments have been conducted by applying the attacks to watermarked Lena image of size 256 × 256, where 2650 bits of information are embedded. The test results show that the proposed watermarking schemes are resistant to various attacks and common image processing operations. The robustness is illustrated with the BER obtained after attacks on watermarked images and is reported in Table 3.

The BERs obtained for the proposed scheme is very negligible when compared to the amount of information embedded. For instance, for median filtering attack on a watermarked of size 256 × 256, with 2650 bits embedded using proposed scheme result in a BER of 2.2. However, for the existing works [1, 6], the resultant BERs are 41.79 and 30.46, respectively, with only 256 bits embedded.

Corresponding to the robustness test results, the following observations are made:

1. *Additive noise:* The proposed approaches are robust to additive white Gaussian noise. Even when the variance is varied from 0.5 to 5, the BER is zero.
2. *Common filtering operation:* The watermark is better robust to median filtering with a mask of size 3 × 3. The BER obtained is negligible when compared to the order of bits embedded. Further, it shows robustness to average and mean filtering also.
3. *Image enhancement operations:* The BERs obtained for sharpening and histogram equalisation are nearly zero, showing the resistance of watermark against those attacks. Further, it holds good for de-correlation stretch (provides visual enhancement to an image with significant band-to-band correlation) and contrast limited adaptive histogram equalisation (CLAHE) which makes image intensity values

Table 3 BERs obtained after attacks on watermarked Lena image WFWLC and existing DWT–DCT watermarking schemes

Serial no.	Attack type	Bit error rate		
		WFWLC scheme	Al-Haj's DWT–DCT scheme	Kasmani *et al.* DWT–DCT scheme
1	no attack	0	0	0.3
2	additive noise	0	50	45.31
3	median filtering	2.2	41.79	30.46
4	de-correlation stretch	0	50	45.31
5	CLAHE	0	14.06	7.03
6	blurring	1.43	41.4	16.4
7	sharpening	0.35	34.37	24.6
8	histogram equalisation	0.52	50	45.31

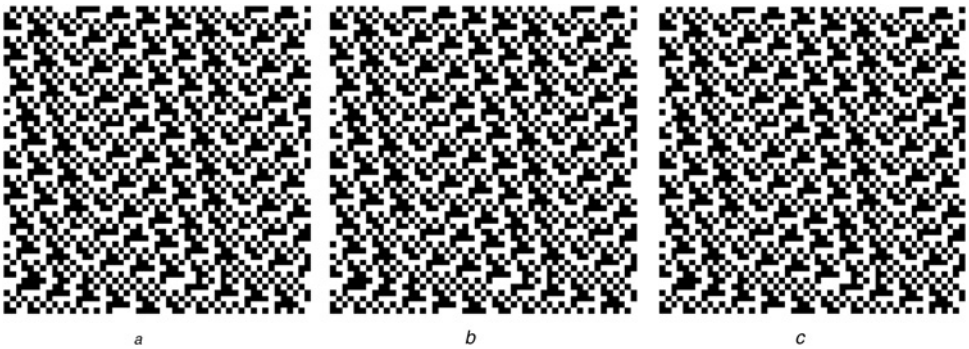

Fig. 8 *Original watermark and the watermarks recovered after attacks on watermarked images*
a Original watermark
b Watermark recovered after additive noise
c Watermark recovered after sharpening attacks

to be evenly distributed throughout the image. Further, the proposed schemes are robust to blurring attacks with a minimal BER. A work related to the blind detection of blurring via edge-based blur estimation has been introduced by Cao *et al.* [22].

From Table 3, it is clear that DWT–FBT watermarking domain is better robust to almost all the common attacks. This robustness is however achieved with the use of FBT in the proposed scheme. Hence, a conclusion can be made that this combined domain is better robust to attacks along with achieving a significant improvement in the quality and capacity of the watermarked image than the existing DWT–DCT watermarking schemes.

Fig. 8 illustrates how the original watermark and the watermarks extracted after attacks on watermarked images would appear with the support of results from Table 3 to give the reader, a better understanding of the watermarking approaches. Fig. 8*a* shows the watermark, which is a binary bit pattern that is embedded; Figs. 8*b* and *c* show the watermark that is extracted after attacks like additive noise and sharpening, respectively, for the WFWLC scheme. However, for the WFWLC scheme, the BER is zero for additive noise attack and this is shown in Fig. 8*b* where the watermark extracted resembles the original watermark. It can also be seen that for sharpening attack, the BER reported by WFWLC is 1.43 which is very negligible when compared to the number of bits embedded and the distortions in the watermark are not clearly seen and this is shown in Fig. 8*c*.

5 Conclusion

The proposed non-blind colour image watermarking schemes in DWT–FBT domain utilise either the chromatic content or both the luminance and chrominance content for watermarking. A significant improvement in PSNR of watermarked images is achieved using both WFWC and WFWLC schemes when compared to DWT–DCT approaches [1, 6]. Further, the proposed schemes have a high data embedding capacity in addition to being imperceptible to human vision. They are robust to attacks like blurring, sharpening and histogram equalisation and find its application in image authentication, copy control and content tracking. It is proposed to develop a blind watermarking scheme with high quality, robustness and data embedding capacity in future.

6 References

1 Al-Haj, A.: 'Combined DWT-DCT digital image watermarking', *J. Comput. Sci.*, 2007, **3**, (9), pp. 740–746

2 Jiansheng, M., Sukang, L., Xiaomei, T.: 'A digital watermarking algorithm based on DCT and DWT'. Proc. Second Int. Symp. on Information Systems and Applications, 2009, pp. 104–107

3 Tripathi, S., Jain, R.C., Gayatri, V.: 'Novel DCT and DWT based watermarking techniques for digital images'. Proc. 18th Int. Conf. on Pattern Recognition, 2006, vol. 4, pp. 358–361

4 Emek, S., Pazarci, M.: 'A cascade DWT-DCT based digital watermarking scheme'. Proc. 13th European Signal Processing Conf., 2005

5 Kang, X., Huang, J., Shi, Y.Q., Lin, Y.: 'A DWT-DFT composite watermarking scheme robust to both affine transform and JPEG compression', *IEEE Trans. Circuits Syst. Video Technol.*, 2003, **13**, (8), pp. 776–786

6 Kasmani, S.A., Nilchi, A.N.: 'Robust digital image watermarking technique based on joint DWT-DCT transformation', *Int. J. Digit. Content Technol. Appl.*, 2009, **3**, (2), pp. 42–54

7 Tsui, T.K., Zhang, X.-P., Androutsos, D.: 'Color image watermarking using multidimensional Fourier transforms', *IEEE Trans. Inf. Forensics Secur.*, 2008, **3**, (1), pp. 16–28

8 Cai, L., Du, S.: 'Rotation, scale and translation invariant image watermarking using radon transform and Fourier'. Proc. IEEE 6th Circuit and Systems Symp. on Emerging Technologies: Mobile and Wireless Communication, 2004, pp. 281–284

9 Rahim, R.A., Rahiman, M.H.F., Chen, L.L., San, C.K., Fea, P.J.: 'Hardware implementation of multiple fan beam projection in optical fiber process tomography', *Sensors*, 2008, **8**, pp. 3406–3428

10 Murry, R.C., Dowdry, J.E., Christensen, E.E.: 'Christensen's physics of diagnostic radiology'1990pp. 1294–1296

11 Dejey, D., Rajesh, R.S.: 'Robust color image watermarking based on fan beam projections', *Int. J. Image Acquis.*, 2009, **6**, (4), pp. 269–280

12 Tao, P., Eskicioglu, A.M.: 'A robust multiple watermarking scheme in the discrete wavelet transform domain', *Proc. SPIE – Int. Soc. Opt. Engng.*, 2004, **5601**, pp. 133–144

13 Battisti, F., Carli, M., Neri, A., Egiazarian, K.: 'Image watermarking in the Fibonacci–Haar transform'. Proc. Int. Workshop on Nonlinear Signal and Image Processing, Bucharest, Romania, 10–12 September 2007

14 Shieh, C.-H., Huang, H.-C., Wang, F.-H., Pan, J.-S.: 'Genetic watermarking based on transform domain techniques', *Patt. Recogn.*, 2004, **37**, (3), pp. 555–565

15 Dejey, D., Rajesh, R.S.: 'An improved wavelet domain digital watermarking for image protection', *Int. J. Wavelets Multiresolution Inf. Process.*, 2010, **8**, (1), pp. 1–13

16 Nagy, A., Kuba, A.: 'Parameter settings for reconstructing binary matrices from fan beam projections', *J. Comput. Inf. Technol. (CIT)*, 2006, **14**, (2), pp. 101–110

17 www.mathworks.com/access/helpdesk/help/toolbox/images/fanbeam.html

18 Bremananth, R., Chitra, A.: 'Real time orientation detection and recognition'. Proc. 1st Int. Conf. on Image and Signal Processing, 2006, vol. 1, pp. 460–466

19 Gonzalez, R.C., Woods, R.E.: 'Digital image processing' (Pearson Education, 2nd edn.), 2002, pp. 419–420

20 USC-SIPI Image Database, http://sipi.usc.edu/services/database/Database.html

21 Phadikar, A., Verma, B., Jain, S.: 'Region splitting approach to robust color image watermarking scheme in the wavelet domain', *Asian J. Inf. Manage.*, 2007, **1**, (2), pp. 27–42

22 Cao, G., Zhao, Y., Ni, R.: 'Edge-based blur metric for tamper detection' *J. Inf. Hiding Multimedia Signal Process.*, 2010, **1**, (1), pp. 20–27

doi: 10.1049/iet-ipr.2009.0239